Carbohydrate Research, 235 (1992) 1–13
Elsevier Science Publishers B.V., Amsterdam

Conformational analysis of β-D-fructofuranosyl-(2 → 6)-β-D-glucopyranoside by molecular mechanics (MM2) calculations *,†

Andrew L. Waterhouse [a], Károly Horváth [b] and Jianhua Liu [b]

[a] *Department of Viticulture and Enology, University of California, Davis, California 95616 (USA)*
[b] *Department of Chemistry, Tulane University, New Orleans, Louisiana 70118 (USA)*

(Received December 2nd, 1991; accepted March 10th, 1992)

ABSTRACT

Conformational energies for models of the disaccharide β-D-fructofuranosyl-(2 → 6)-β-D-glucopyranoside were computed by molecular mechanics using MM2(87). An initial investigation of staggered forms examined the linkage bonds characterized by the torsion angles ϕ, ψ, and ω, and subsequently the fructose hydroxymethyl side groups, characterized by the torsion angles χ-1 and χ-6. Then, in our major search of conformational space, the torsion angles of two linkage bonds, ϕ and ω, were driven through 360° in 20° increments at all staggered side group combinations. From these results, the low-energy forms were minimized without the driver restrictions to generate the global minimum structure found and herein reported. This conformer was then used to map the conformational space of ϕ and ω by driving only those torsion angles through 360°. Both the ${}^{4}_{3}T$ (northern) conformer (Cremer–Pople puckering phase angle of $\phi_2 = 265°$) and the ${}^{3}_{4}T$, (southern) conformer ($\phi_2 = 80°$) of the fructofuranose ring were tested for comparison, and both were shown to be significant contributors of populated forms. As these two conformers had different minima for a number of important torsion angles, experimental studies may reveal different properties than those expected solely from the preferred northern conformer.

INTRODUCTION

The fructans belong to a group of poly- and oligo-saccharides in which fructofuranose units predominate[1], usually with a terminal glucopyranose unit. They occur in some plants[2], and their occurrence appears to be related to cold tolerance[3]. A better understanding of the structure of these sugars will help studies of their mechanism of action in the plant. The simplest common fructans are the kestoses (fructofuranosyl derivatives of sucrose), namely, 1-kestose, 6-kestose, and

Correspondence to: Dr. A. Waterhouse, Department of Viticulture and Enology, University of California, Davis, CA 95616, USA.

* Paper No. 6 of a series: Conformational Analysis of D-Fructans.

† This paper is dedicated to the memory of Professor Márton Kajtár (deceased, June 21st, 1991).

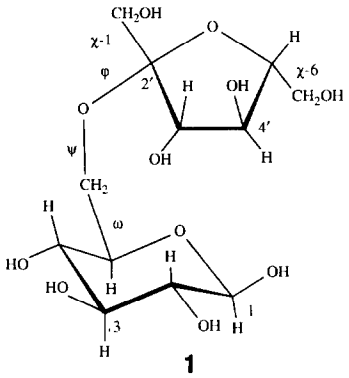

Fig. 1. β-D-Fructofuranosyl-(2 → 6)-β-D-glucopyranoside (**1**). ϕ = C-6–O–C-2′–O-5′, ψ = C-5–C-6–O–C-2′, ω = O-5–C-5–C-6–O, χ-1 = O-1′–C-1′–C2′–O-5′, χ-6 = O-6′–C-6′–C-5′–O-5′.

neokestose. The disaccharide studied here, β-D-fructofuranosyl-(2 → 6)-β-D-glucopyranoside (**1**), is a constituent of the trimer neokestose.

This disaccharide (**1**, Fig. 1) has been known in the literature since the early 1950s as a product of various enzymatic transfructosylation reactions. Its characterization, however, is far from being complete. Most reports present little or no reproducible physical data, i.e., spectroscopic data, and the most common parameter, optical rotation, has been the subject of contradictory reports.

Whelan and Jones published the first report on **1** by observing its formation by yeast acting on sucrose. They established the structure by chemical methods as β-D-fructofuranosyl-(2 → 6)-β-D-glucopyranoside[4]. Bacon[5] and Bell and Edelman[6] also observed the formation of **1** in the reaction of sucrose with yeast invertase, whereas Hestrin and coworkers reported **1** as a product in the enzymic reaction of sucrose with levansucrase[7,8].

Bochkov and Kochetkov reported on the first synthesis of **1** in 1969. (ref. 9). They characterized it with an optical rotation of +7° (*c* 1.4, H_2O). In a 1970 paper, Arcamone[10] reported **1** as a product of a strain of *Claviceps purpurea*; however, the only physical data reported was an optical rotation ($[\alpha]_D$ = +1.0°, H_2O, equilibrium) which differed from other published data. However, Arcamone supplied the sample of **1** for Kamerling and coworkers' mass spectroscopic investigation that confirmed the proposed structure[11,12].

Among other carbohydrates in wine must, **1** was mentioned under the name of neokestobiose[13]. A disaccharide named ceratose[14] was isolated from the fruit of St. John's bread (*Ceratonia siliqua* L.) which is a fructofuranosyl glucoside; however, the linkage between the monosaccharide units is uncertain, and the reported optical rotation ($[\alpha]_D^{23}$ = +21°, *c* 2.8, H_2O) is again different from those values mentioned above. Straathof et al.[15] reported a small amount of **1** from the action of invertase isolated from yeast (*Saccharomyces cerevisiae*) on concentrated sucrose

solution. There are other reports with fragmentary evidence to support the presence of **1** (ref. 16).

In the second and fifth paper of this series, the conformational features of inulobiose[17] and levanbiose[18] were studied by the MM2 method. Herein we report the results of an MM2 study of **1**, which in combination with studies on sucrose[19] will encompass all disaccharides found in the kestoses as well as in most fructans. We have modeled the isolated molecule to obtain information about the energetically most likely conformations of this disaccharide by computing its steric energies at different torsion angles of the central linkage bonds, namely, the ϕ, ψ, and ω angles, as well as at the staggered angles of the side groups. Although currently no experimental data are available to corroborate these theoretical data, related structures, i.e., neokestose, may well serve as a base for experimental comparison. In solution, **1** most likely exists as a mixture of α and β anomers, and that will complicate experimental analysis.

COMPUTATIONAL DETAILS

Initial structures were created graphically using PCMODEL (version 4.0) [Serena Software, Bloomington, IN 47402 (USA)] on a personal computer, and after structural minimization this program was used to create MM2 input files. Editing was required to accommodate our modifications of MM2(87), and these files were used as the input for MM2(87) calculations on IBM Risc System 6000-540. The default convergence criteria of $\Delta E = N \times 0.00008$ kcal/mol was applied in the minimization computations where N is the number of atoms in the molecule; smaller criteria as low as 0.00002 resulted in no significantly lower energies. Only the "−2" dihedral angle driver was used[17]. Runs which carried out 144 minimizations took approximately four hours to complete.

The side-group staggered forms can be described using the *gauche/trans* (g/t) system, where the first letter describes the relative position of the side-group oxygen to the ring oxygen (O-5), and the second to C-4. Specifically, $gg = -60°$, $gt = 60°$, and $tg = 180°$, where the torsion angles are described by the side-group oxygen and the ring oxygen.

Modeling with the ${}^{4}_{3}\mathrm{T}$ *(northern) fructofuranose ring conformation.*—The analysis of **1** was started by constructing an initial model consisting of a fructofuranose unit in its most stable form, the ${}^{4}_{3}T$ conformation ($\phi_2 = 265°$)[20], and a glucopyranose unit of the ${}^{4}C_1$ chair conformation with the linkages listed in Table I, structure **i**. Energy minimization of this structure in MM2 (Run 1) resulted in **ii**. Using **ii** as the starting structure, we then carried out a preliminary search for low-energy forms, looking first at linkage angles and then side groups in turn. The linkage bonds (ϕ, ψ, ω) were driven through all staggered conformations in 120° steps, (Run 2). The structure of the lowest energy conformation, **iii**, was allowed to fully relax (Run 3), giving **iv**. This conformation was used as the starting point for a

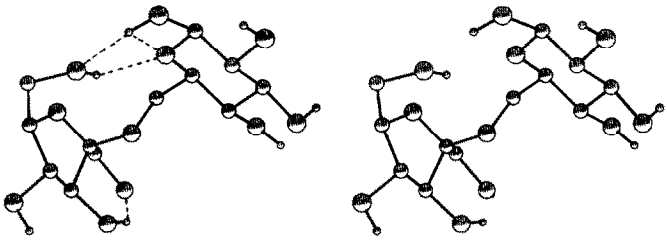

Fig. 2. Stereoview of the global minimum structure **vii** found in this study. H-bonds are indicated by dashed lines.

side-group search of staggered forms, Run 4, and again the lowest energy form, **v**, was reoptimized with no restrictions to yield **vi** (Run 5).

Using **vi**, a full search of both side-group and linkage conformational space was carried out for Runs 6–14 (excluding ψ). In each survey, the side groups were placed in a different staggered form (9 in all), and the linkage angles ϕ and ω were driven through 360° in 30° increments. From each survey, the 10 lowest

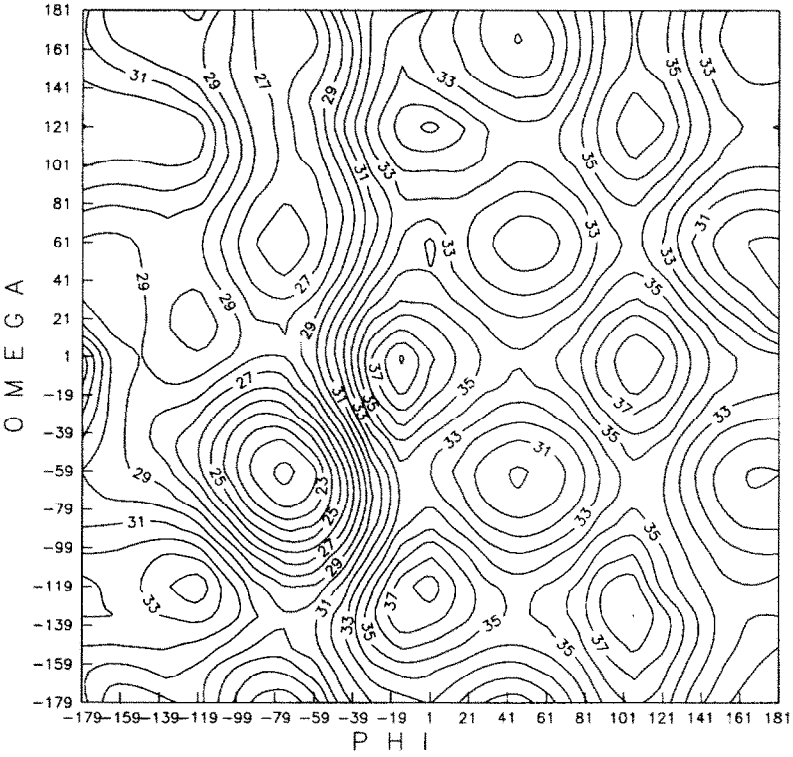

Fig. 3. A contour map of the relaxed steric energy (kcal/mol) for **1** at combinations of ϕ and ω for the ${}^{4}_{3}T$ fructofuranose form (Run 16).

TABLE I

Torsion angles of each of the lowest-energy structures found in each run with ring conformation ^4_3T

	Conformer	Angle (deg)					Energy (kcal/mol)	Type of Analysis
		ϕ	ψ	ω	χ-1	χ-6		
	i	−155.9	169.9	179.5	64.0	−60.9		initial structure
Run 1	**ii**	−149.4	176.9	170.3	56.8	−62.8	31.7	MM2 minimized
Run 2	**iii**	−61.1	178.8	−61.0	44.7	−70.7	25.4	linkage-staggered forms
Run 3	**iv**	−70.8	159.1	−59.2	49.0	−59.8	21.7	fully relaxed **iii**
Run 4	**v**	−79.5	162.2	−59.4	−176.3	−59.4	20.3	side-group staggered forms
Run 5	**vi**	−74.1	161.6	−59.1	−177.5	−60.5	20.2	fully relaxed **v**
Run 6–14	Mapping ϕ/ψ conformational space with rigid side groups, see Table II.							
Run 15	**vii**	−75.9	160.8	−61.4	−176.6	−59.6	20.2	global minimum
Run 16	Mapping ϕ/ψ conformational space in 20° increments. See Fig. 3, Table IV.							

energy forms were extracted (Table II), and their structures were reminimized (Run 15) allowing all the driven angles to relax. Those are tabulated only for Run 8 (Table III) which yielded **vii**, the global minimum found here (Fig. 2).

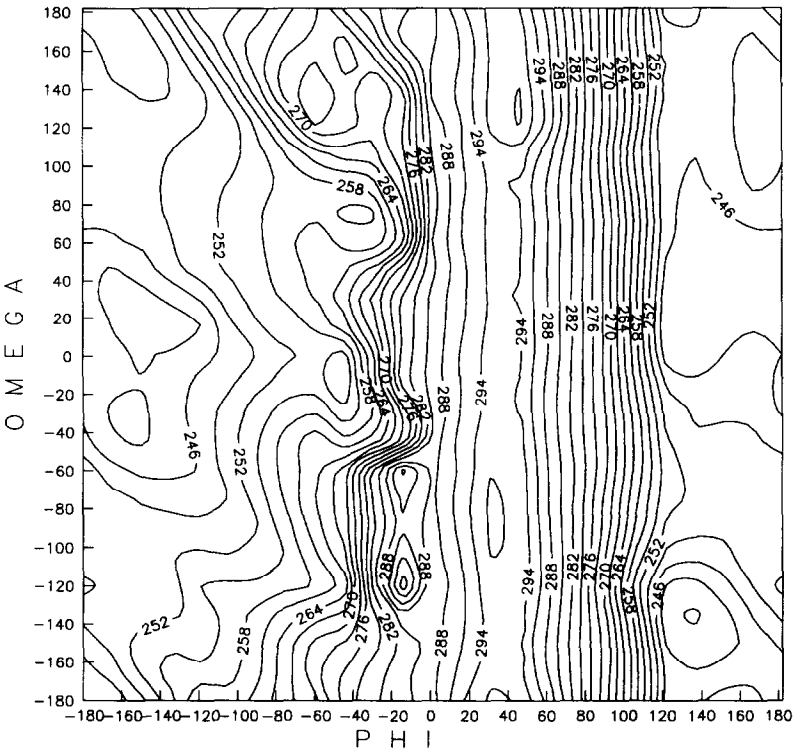

Fig. 4. A contour map of the fructofuranose ring-puckering value on the Cremer–Pople scale at combinations of ϕ and ω (Run 16).

TABLE II

Energies and angles from the angle-driving runs (6–14) of angles ϕ and ω. The top ten low-energy structures of each run are shown

Side-group position	Angle (deg)					Energy (kcal/mol)
	ϕ	ψ	ω	χ-1	χ-6	
gg-gg	−59.8	156.1	−59.7	−69.6	−61.3	24.32
Run 6	−89.7	165.1	−59.7	−70.1	−59.3	24.35
	−59.8	155.9	−89.6	−69.3	−58.3	26.55
	−89.7	162.6	−29.7	−70.3	−62.5	26.81
	−59.7	162.1	151.1	−64.8	−56.5	27.11
	−29.8	125.6	−59.7	−58.7	−57.1	27.54
	−59.8	158.3	−179.0	−64.9	−60.5	27.54
	−89.6	167.0	−89.6	−70.3	−57.7	28.32
	−59.9	149.4	−29.8	−69.3	−62.5	28.42
	−119.8	175.0	−59.6	−67.5	−58.9	28.53
gt-gg	−59.8	153.1	−59.7	51.9	−60.0	22.29
Run 7	−89.7	164.9	−59.7	50.6	−59.3	22.70
	−59.7	153.3	−89.6	52.7	−58.0	24.30
	−89.7	162.7	−29.7	50.1	−62.0	25.25
	−89.7	167.4	−89.7	51.1	−58.0	25.92
	−59.8	144.6	−29.8	53.4	−61.0	26.04
	−29.8	127.4	−59.7	61.9	−58.9	26.69
	−59.7	158.4	60.7	52.7	−53.6	26.80
	−89.7	171.9	−178.9	51.3	−59.6	26.93
	−59.7	160.7	151.1	52.4	−56.3	26.94
tg-gg	−89.7	163.5	−59.7	−173.8	−58.9	21.22
Run 8	−59.8	157.3	−59.7	−175.5	−62.8	21.44
	−89.7	161.7	−29.7	−174.0	−62.0	23.62
	−59.8	156.7	−89.6	−175.3	−59.7	23.72
	−89.6	165.4	−89.6	−174.1	−57.4	25.12
	−59.9	152.2	−29.8	−175.9	−64.1	25.51
	−89.7	166.3	60.7	−173.7	−56.5	25.63
	−199.8	174.9	−59.6	−167.3	−59.3	25.85
	−59.8	160.1	60.7	−175.7	−55.6	25.95
	−59.7	159.0	90.8	−175.6	−60.2	26.19
tg-gt	−59.8	162.4	−59.7	−174.1	63.9	27.34
Run 9	−89.7	165.6	−59.7	−172.9	63.9	27.72
	−59.8	162.6	60.7	−174.3	65.2	28.17
	−89.7	165.2	60.7	−173.2	65.7	28.59
	−59.8	162.1	−89.7	−174.2	63.3	28.73
	−59.8	164.5	−179.0	−176.9	64.6	29.44
	−89.7	166.5	−89.7	−173.3	64.6	29.53
	−29.7	−178.6	−59.7	−169.4	62.2	29.69
	−59.8	163.0	30.7	−174.6	64.7	29.75
	−59.7	165.5	151.1	−177.0	66.4	29.79
gg-gt	−59.8	162.6	−59.7	+71.3	63.5	30.33
Run 10	−29.7	178.2	−178.9	−61.2	62.4	30.33
	−89.7	167.3	−59.7	−69.8	63.3	30.99
	−59.8	162.9	60.7	−71.5	64.9	31.36
	−59.8	162.5	−89.7	−71.0	63.0	31.71

TABLE II (continued)

Side-group position	Angle (deg)					Energy (kcal/mol)
	ϕ	ψ	ω	χ-1	χ-6	
gg-gt	30.6	163.8	−179.0	−60.9	64.1	31.91
Run 10	−89.7	166.9	60.7	−69.9	65.2	32.00
	30.7	158.0	−59.7	−60.8	63.8	32.04
	0.4	168.2	−179.0	−59.5	61.4	32.21
	0.5	166.5	151.1	−59.3	62.2	32.31
gt-gt	−59.8	161.7	−59.7	50.7	64.1	28.89
Run 11	−89.7	167.3	−59.7	51.4	63.8	29.56
	−59.7	164.0	−178.9	52.0	64.6	29.76
	−59.7	161.5	60.7	53.0	65.7	29.94
	−29.6	173.0	−178.9	61.8	63.5	29.94
	−59.7	161.6	−89.7	51.4	63.4	30.04
	−59.7	163.7	151.1	52.8	66.4	30.55
	−89.7	168.6	−89.7	52.0	64.4	30.80
	−89.7	168.2	60.7	52.2	65.7	30.81
	−59.7	165.9	−150.1	52.1	65.2	30.83
gt-tg	−59.7	160.0	−59.7	51.0	178.0	27.78
Run 12	−59.7	162.7	−178.9	51.8	177.2	28.52
	−29.6	173.6	−178.9	61.6	177.1	28.58
	−59.7	159.3	60.7	53.1	177.2	28.59
	−89.7	166.7	−59.7	51.1	177.1	28.82
	−59.7	162.3	151.1	52.8	177.4	29.01
	−59.7	160.1	−89.7	51.7	177.3	29.17
	−89.7	169.3	60.7	51.9	176.9	29.46
	−59.7	164.4	−150.1	52.4	177.5	29.55
	−29.7	179.6	60.7	62.0	176.4	29.73
tg-tg	−59.8	160.8	−59.7	−174.3	177.4	26.39
Run 13	−89.7	163.9	−59.7	−173.6	176.7	27.15
	−59.8	160.8	60.7	−174.9	176.8	27.20
	−89.7	163.6	60.7	−173.8	176.5	27.62
	−59.8	160.3	−89.7	−174.5	176.7	28.07
	−59.8	162.7	−179.0	−177.0	176.5	28.35
	−59.7	163.3	151.1	−177.1	176.5	23.38
	−29.7	−177.2	−59.7	−169.6	175.6	28.46
	−59.8	161.3	30.7	−175.2	176.8	28.89
	−59.8	160.9	90.7	−174.5	176.4	28.96
gg-gt	−29.6	−179.4	−178.9	−61.4	177.6	29.12
Run 14	−59.8	161.5	−59.7	−71.7	177.8	29.34
	−59.8	161.6	60.7	−72.0	177.2	30.30
	−89.7	166.3	−59.7	−70.0	177.1	30.36
	30.6	163.9	−179.0	−61.4	178.1	30.74
	−89.7	165.5	60.7	−70.2	176.8	30.99
	−59.8	161.2	−89.7	−71.4	177.2	30.99
	30.7	160.5	−59.7	−61.9	178.1	31.04
	0.4	168.1	−179.0	−59.7	176.6	31.05
	0.5	166.8	151.1	−59.5	177.5	31.11

TABLE III

Run 15: torsion angles, ring-puckering angle, and energies obtained by fully relaxed optimization of the 10 low-energy structures of Run 8, reordered based on energy. Note that the top 7 structures are essentially the same

Angle (deg)						Energy (kcal/mol)
ϕ	ψ	ω	χ-1	χ-6	ϕ_2	
−75.9	160.8	−61.4	−176.6	−59.6	259	20.26
−73.9	161.5	−58.1	−176.7	−61.0	259	20.31
−73.3	162.0	−57.7	−176.8	−61.2	259	20.33
−76.7	159.5	−63.8	−176.4	−59.1	260	20.35
−76.7	159.7	−64.0	−176.5	−59.1	260	20.35
−76.7	159.5	−63.8	−176.4	−59.1	260	20.35
−73.3	162.0	−57.7	−176.8	−61.2	260	20.35
−73.4	166.0	66.3	−177.2	−56.7	256	25.02
−79.4	164.9	54.9	−176.3	−56.7	255	25.04
−65.1	158.6	94.1	−176.5	−59.3	257	25.98

Starting with **vii**, a study of its ϕ/ω conformational space was carried out by driving only ϕ and ω in 20° increments (Run 16). The energy at each value of ϕ and ω was ascertained, and a contour map of the energy was created from this survey (Fig. 3). A tabulation of the 10 lowest energy points from the survey is presented in Table IV. In addition, a map of the fructofuranose ring puckering using the Cremer–Pople ϕ_2 angle[21] was compiled at each ϕ/ω value (Fig. 4).

Modeling with the ${}^{3}_{4}$T *(southern) fructofuranose ring conformation.*—In this case, a somewhat different preliminary study produced a good starting model. Then a survey of all combinations of the two linkage angles, ϕ and ω, and the two side groups was obtained by testing all their staggered forms to determine the energy of

TABLE IV

The 10 low-energy conformations of Run 16 with their linkage torsion angles and ring-puckering phase angles (ϕ_2), all points are plotted in Fig. 3

Angle (deg)						Energy (kcal/mol)
ϕ	ψ	ω	χ-1	χ-6	ϕ_2	
−79.55	162.22	−59.49	−176.33	−59.42	258.5	20.31
−59.63	158.07	−59.52	−175.61	−63.18	262.8	21.50
−79.58	161.64	−39.51	−176.53	−62.20	257.0	21.79
−79.52	162.30	−79.46	−175.15	−58.41	256.5	21.87
−59.58	157.91	−79.47	−175.28	−60.85	263.6	22.28
−99.54	166.58	−59.46	−171.13	−58.82	251.6	22.62
−99.57	165.79	−39.49	−171.03	−60.68	251.8	23.44
−59.68	154.01	−39.55	−175.88	−64.07	262.7	23.76
−99.50	168.16	−79.44	−171.27	−57.77	248.7	24.95
−79.58	165.01	61.08	−176.33	−56.42	256.0	24.98

TABLE V

The torsion angles and energies of the 10 lowest-energy structures from Run 17, the survey of all staggered forms of ϕ, ω, χ-1 and χ-6, on the $^{3}_{4}T$ form

Angle (deg)					Energy (kcal/mol)
ϕ	ψ	ω	χ-1	χ-6	
59	−154	59	179	59	23.0
59	−155	59	59	59	24.2
59	−162	−61	179	59	24.4
59	−154	59	−61	59	25.4
59	−162	−61	59	59	25.7
59	−161	−61	179	179	26.1
59	−167	59	179	179	26.6
59	−160	−61	−61	59	26.8
59	−162	−61	59	179	27.4
179	−162	−61	−61	59	27.8

81 structures (Run 17). The 10 lowest energy forms are listed in Table V. Each of these structures was minimized without restrictions (Run 18), producing the energy minimum structure, **viii**, 21.9 kcal/mol (Table VI). Structure **viii** was used to

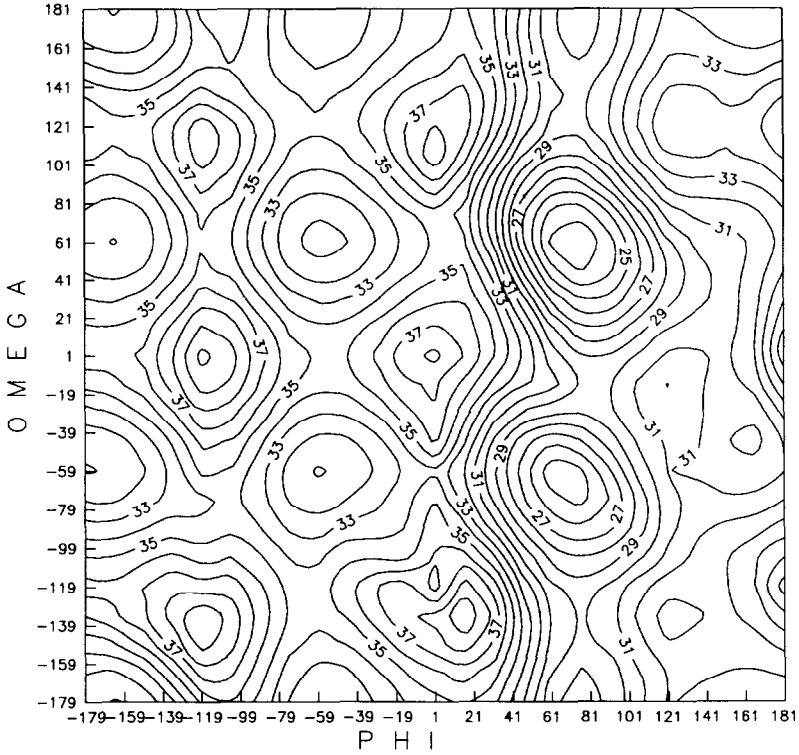

Fig. 5. A contour map of the relaxed steric energy (kcal/mol) for **1** at combinations of ϕ and ω for the $^{3}_{4}T$ fructofuranose form (Run 19).

TABLE VI

Results from Run 18. Torsion angles, puckering angles and energies were obtained by fully relaxed optimization of the 10 conformers listed in Table V, and are tabulated in the same order

Angle (deg)						Energy (kcal/mol)
ϕ	ψ	ω	χ-1	χ-6	ϕ_2	
72.3	−161.3	57.0	−176.1	63.1	80.5	21.9 [a]
71.5	−160.0	57.6	55.8	62.2	83.0	23.2
70.6	−168.9	−66.3	−176.0	57.6	87.2	23.6
72.1	−162.1	58.6	−45.9	63.3	80.3	23.5
69.9	−167.0	−66.3	56.1	56.9	90.3	25.0
68.4	−167.4	−63.0	−175.6	176.0	83.7	25.3
66.3	−164.6	55.4	−176.1	175.4	77.6	26.1
70.4	−169.6	−66.4	−39.5	58.2	87.2	24.8
67.1	−165.7	−63.1	55.9	175.8	86.7	26.8
−177.8	−162.7	−64.2	−67.6	59.8	67.3	27.5

[a] Conformer **viii**.

directly map ϕ/ω conformational space (Run 19) as above (Run 16), see Fig. 5. The fructofuranose ring form maintained its $^{3}_{4}T$ form during Run 19.

RESULTS AND DISCUSSION

Our initial study was designed to find a low-energy structure that would be a good starting point for further work, as well as help eliminate variables which were not important. In the (2 → 6)-β-linked disaccharides, the geometry of the linkage can be best characterized by the torsion angles ϕ, ψ, and ω. Initially we varied all the three torsion angles to find the energetically most favorable combinations for subsequent surveys. We found, as we have found with other three-bond disaccharide linkages, that the central bond, ψ, is virtually always found in the antiperiplanar form and other variables were more important. In the subsequent studies, ψ always was set to $\approx 180°$ and allowed to relax. A preliminary, cursory study of the orientations of the glucose secondary hydroxyl groups[22] indicated that the orientation where HO-2 points at the ring oxygen, reverse clockwise was preferred, and this orientation was used throughout.

We were also able to shorten our initial survey by looking at side-group positions as a secondary factor. In that study we looked only at the different side-group orientations on our linkage-minimized structure, **iv** (Table I). Although the side groups are a secondary factor, we did find that a different combination of side-group orientations lowered the energy significantly by 1.4 kcal/mol (**vi**). When all the variables were studied simultaneously, we found essentially the same structure as **iv** for the global minimum. This seems to indicate that, while side-group orientation can affect energy, the interresidue H-bonds are not the most important here. After comparing the models, we can suggest two reasons for this effect.

First, the most important factor in defining interresidue geometry is the reduction of interresidue steric strain. When this demand is met with three-bond

linkages, the two residues are generally separated quite well. As a result, there is limited opportunity for multiple interresidue H-bonds to form. Second, when interresidue H-bonds do form, their strength is often attenuated by intraresidue H-bonds.

On examining the ϕ/ω map in Fig. 3, it appears that the linkage is populated only at $\phi = -60°$ and $\omega = -60°$. To see if the side-group orientation would affect this general trend, we looked through Table 2 which lists all the low-energy forms for all combinations of side-group forms, but found that most conformers listed had the $-60°$ orientation for ϕ and ω, with just a few cases of $\omega = 180°$ appearing up to 5 kcal/mol above the minimum.

Table III clarifies the situation further. When the 10 lowest energy structures of Run 8 were minimized without the drivers in place, they collapsed to the **vi** form (20.2 kcal/mol) and two other forms at 25.0 and 26.0 kcal/mol. So, clearly, the 60° angle instead of $-60°$ at ω costs roughly 5 kcal/mol, meaning that one would expect only 0.05% of this form.

However, when the fructofuranose ring has the southern conformer, the major valley is at $\phi = 75°$ and $\omega = 60°$ as shown in Fig. 5. This minimum of this valley for the ${}^{3}_{4}T$ form, **viii**, is only 1.5 kcal above the global minimum, and so it will be populated at $\sim 10\%$ that of the global minimum. (This assumes that the energetic valleys at the two minima are similar in degree of concavity, which appears to be the case, comparing Figs. 3 and 5.) It is interesting to note that the energy difference between **viii** and the global minimum, **vii**, 1.5 kcal/mol, is similar to the energy difference between the southern and northern fructofuranose conformers in the monomer[20].

Consequently, in an experimental situation where one would expect to see conformational flexibility, such as in solution, it seems likely that physical properties would exhibit small but possibly significant effects from the **viii** form.

The behavior of one side group appears similar. In the northern, ${}^{4}_{3}T$ form, the χ-6 torsion angle has a very strong preference for the *gg* form; from Table II, other rotamers cost at least 6 kcal/mol. But, the southern ${}^{3}_{4}T$ form has a different preference. The χ-6 angle shows a marked preference for *gt*. So, physical studies may reveal flexibility at χ-6 due to the presence of the ${}^{3}_{4}T$ form. On the other hand, χ-1 is much more flexible, with the *tg* and *gt* forms within 1 kcal/mol when the ring has the northern form.

The Cremer–Pople puckering phase angles (ϕ_2) were monitored during the calculations. As shown in Fig. 4, ring puckering was affected only moderately by the linkage torsion angle; the ring never was distorted out of its northern form. The same was true for the southern conformer.

CONCLUSIONS

The conformational analysis of **1** has shown that this molecule, as it was anticipated on the basis of other oligosaccharide studies, is rather flexible. It is

very important to note that its flexibility at linkage bonds and at side groups is based on the presence of different fructofuranose ring forms. The preferred ring conformation, ${}^{4}_{3}T$, furnished, as expected, the global minimum for this study, although it is possible that a lower energy form exists. However, we could not sample all conformational space. The other ring conformation, ${}^{3}_{4}T$, also led to an accessible structure. Because this other ring conformer also contained different linkage and side-group angles, physical studies should reveal either (1) the presence of more than one form for the affected linkage and side group angles, or (2) different averaged properties for these same entities, as in NMR spectroscopy, than would be expected from just the northern conformer. This is different from our modeling study of 1-kestose, where different ring forms did not affect the linkage angles[23]. However, this result points to the necessity of considering the southern ring form when studying the structure of fructofuranose-containing compounds.

ACKNOWLEDGMENTS

We thank the office of the Vice Chancellor-Research at the University of California, Davis for financial support, as well as the Computing Services at both Tulane and UC Davis for computer time and courteous assistance.

REFERENCES

1 A.D. French, *J. Plant Physiol.*, 134 (1989) 125–136.
2 C.J. Pollock and N.J. Chatterton, in J. Preiss (Ed.), *The Biochemistry of Plants*, Vol. 14, Academic Press, Boca Raton, FL, 1988, pp 109–140.
3 H.G. Pontis, *J. Plant Physiol.*, 134 (1989) 148–150.
4 W.J. Whelan and D.M. Jones, *Biochem. J.*, 54 (1953) xxxiv.
5 J.S.D. Bacon, *Biochem. J.*, 57 (1954) 320–328.
6 D.J. Bell and J. Edelman, *J. Chem. Soc.*, (1954) 4652–4654.
7 S. Hestrin, D.S. Feingold, and G. Avigad, *Biochem. J.*, 64 (1956) 340–351.
8 D.S. Feingold, G. Avigad, and S. Hestrin, *Biochem. J.*, 64 (1956) 351–361.
9 A.F. Bochkov and N.K. Kochetkov, *Dokl. Akad. Nauk SSSR*, 189 (1969) 1249–1251; *Proc. Acad. Nauk SSSR*, (1969) 987–989.
10 F. Arcamone, W. Barbieri, G. Casinelli, and C. Pol, *Carbohydr. Res.*, 14 (1970) 65–71.
11 J.P. Kamerling, J.F.G. Vliegenthart, J. Vink, and J.J. de Ridder, *Tetrahedron Lett.*, (1971) 2367–2370.
12 J.P. Kamerling, J.F.G. Vliegenthart, J. Vink, and J.J. de Ridder, *Tetrahedron*, 28 (1972) 4375–4387.
13 M. Castino, *Vini Ital.*, 14 (1972) 383–390.
14 K. Wallenfels and J. Lehmann, *Chem. Ber.*, 90 (1957) 1000–1007.
15 A.J.J. Straathof, A.P.G. Kieboom, and H. van Bekkum, *Carbohydr. Res.*, 146 (1986) 154–159.
16 G. Avigad, R. Zelikson, and S. Hestrin, *Biochem. J.*, 80 (1961) 57–61; S. Hestrin and G. Avigad, *Biochem. J.*, 69 (1958) 388–398; S. Sugii and E.A. Kabat, *Carbohydr. Res.*, 82 (1980) 113–124; J. Cisar, E.A. Kabat, M.M. Dorner, and J. Liao, *J. Exp. Med.*, 142 (1975) 435–55; S. Peat, W.J. Whelan, and J.G. Roberts, *J. Chem. Soc.*, (1956) 2258–2260.
17 T.M. Calub, A.L. Waterhouse, and A.D. French, *Carbohydr. Res.*, 207 (1990) 221–235.
18 J. Liu and A.L. Waterhouse, *Carbohydr. Res.*, 232 (1992) 1–15.

19 C.H. du Penhoat, A. Imberty, N. Roques, V. Michon, J. Mentech, G. Descotes, and S. Perez, *J. Am. Chem. Soc.*, 113 (1991) 3720–7; V.H. Tran and J.W. Brady, *Biopolymers*, 29 (1990) 961–976; V.H. Tran and J.W. Brady, *Biopolymers*, 29 (1990) 977–997.
20 A.D. French and V. Tran, *Biopolymers*, 29 (1990) 1599–1611.
21 D. Cremer and J.A. Pople, *J. Am. Chem. Soc.*, 97 (1975) 1354–1355.
22 A.D. French, V.H. Tran, and S. Peréz, *ACS Symp. Ser.*, 430 (1990) 191–212.
23 A.L. Waterhouse, T.M. Calub, A.D. French, *Carbohydr. Res.*, 219 (1991) 29–42.